

# Fracture pattern analysis of hardrock hydrogeological environment, Kea Island, Greece

V. Iliopoulos, S. Lozios, E. Vassilakis, G. Stournaras

<sup>1</sup> Faculty of Geology and Geoenvironment, National & Kapodistrian University of Athens, Department of Dynamic Tectonics and Applied Geology, Panepistimioupolis Zografou, 15784 Athens - Greece, viliopoulos@geol.uoa.gr

**Abstract** The geological and hydrogeological regime of Kea Island is presented, focusing on the fracture pattern analysis of the crystalline-schist mass outcrops the island. The combined use of field mapping and geological data digital analysis extracting lineament density maps and fracture intersection density maps reveals a high relationship between the fracture pattern and the groundwater occurrence. In order to obtain a complete description of the fracture network, the study area is mapped at various scales with the aid of GIS and remote sensing techniques were integrated along with the data gathered from field work. Remarkable correlations between the hydrochemical data of the main springs (located along the SE and NW part of the island), and the results of lineament analysis and the hydro-lithological regime of Kea Island, contribute to extract an integrated conception for the relation of the groundwater potential with the structure of fissured rocks.

## 1 Geology and Tectonic setting

Kea Island belongs to the Attic-Cycladic Belt which is characterized by a complicated deformational and metamorphic development from Late Cretaceous up to present times (Fig. 1). This tectono-metamorphic history involves a Late Cretaceous –Eocene high pressure/low temperature metamorphism followed by a Late Oligocene–Miocene greenschist to amphibolites facies overprint, coeval with the Aegean (post-) orogenic extension (Durr et al. 1978; McKenzie 1978; Altherr et al. 1982). The mid- to late Miocene magmatic activity in the Attic-Cycladic core complex is also closely related to the large-scale extension of the Aegean Arc during this period (Liati et al. 2009).

The island of Kea represents the northernmost island of the Western Cyclades island. According to Iglseider et al. (2008), two tectonostratigraphic units have been identified, separated by a low-angle normal fault-zone (shear zone): i) the lower unit, which occupies almost the whole island and corresponds to the foot-wall block and ii) the upper unit, in the form of sparse relics at the northern part of the island, which corresponds to the detachment itself.

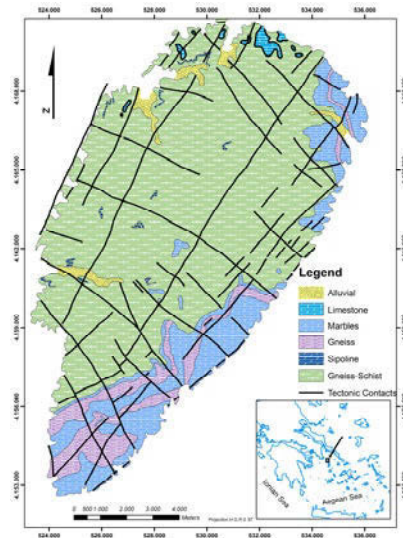


**Fig. 1.** Geological map of Kea Island (Davis 1982).

The footwall, which has a structural thickness of 380>m, predominantly comprises of chloritic schists with lithologically lensoid variations in quartz, carbonate, epidote, actinolite, biotite and talc. Near the detachment zone, talc is locally more common and is associated with small serpentine bodies, dolomite and magnetite-garnet glaucophane schists. All these lithological types are equivalent to the gneiss-schist formation of the previously published geological map (IGME, Davis 1982). Along the SE part of the island, the chloritic schists are interbedded with blue-grey calcite marbles and thin quartz layers Iglseider et al. (2008) and corresponds to the marbles with gneiss-schist intercalations. The upper unit is mainly represented by a 100 m thick zone of tectonic related rocks and is preserved in sparse small klippen up to approximately one square kilometer in size. Calcite ultramylonit and protoclastic dolomite (locally strongly ankeritised) near the fault zone are overlay by weakly deformed dolomite and limestone with occasional ultramylonitic calcitic shear zones (Muller 2009). This upper unit is equivalent with the Triassic-Jurassic carbonate formation. In general, from the hydrogeological point of view, the crystalline complex of Kea Island can be separated in two main groups: i) gneiss-schist group and ii) alternations of marbles and gneiss-schist.

The tectonic structure of Kea Island is dominated by an antiformally domed low-angle normal fault system within a high strain shear zone, cropping out across the whole island and formed during green-schist facies metamorphic conditions (Müller et al. 2007). Isoclinal refolded sheath-type folds and a strongly expressed NNE-SSW stretching lineation, represent the ductile deformation structures during these conditions, showing a top-to-SSW sense of shear. This event followed by at least two phases of brittle deformation, dominated by high-angle normal faults and a population of fractures and joints. Field observations show that the varying orientations of faults and other fractures and the cross-cut relations between different sets, indicate different generations and multiple reactivation periods. Some of them are open, some are bearing angular breccias of the host rock and some others are infilled by ore-rich fluids, quartz, calcite etc. The length, the number and the density of the fractures varies from place to place and in some cases highly fractured zones are cutting the crystalline mass, representing the cataclastic domain of a probable fault-rock zone. The detailed analysis of results of the brittle deformation and the related structures is very important for understanding the hydrogeological environment of Kea Island, comprising a work in progress.

## **2 Hydrogeological setting**

The metamorphic rocks of Kea Island (mainly schists and gneisses with some intercalations of marbles at the SE part) are in general permeable due to the fragmentation that characterizes them. The groundwater flow seem to follow selective paths associated with the fragmentation and the intercalation of carbonate horizons. Furthermore the hydrolithological conditions for the carbonate rocks are characterized by high degree of karstification. The particularities of fissured rocks affect the vulnerability assessment and the risk mapping, as well their role in the framework of an ecohydrological consideration (Stournaras 2008). The alimentation of these formations depends only on the infiltration from the rain precipitation and the discharge is manifested by the springs. Although rocks like gneiss and schist typically are characterized of compact structure, the brittle deformation produce fractured, fissured and cataclastic formations that allow the groundwater flow and infiltration, along the discontinuities.

## **3 Hydrochemical setting**

The groundwater generally flows in a limited depth in Keas' crystalline complex and this water comes out through springs (Fig. 2a). At northern Kea, the overdrilling during decades combined with the low precipitation led to the sea intrusion and the high salinity of the deeper aquifer of crystalline complex. According

Schoeller's diagram the spring water samples (Yannatos 2003) are characterized of high concentrations in Cl, HCO<sub>3</sub> and Ca (Fig. 2b).

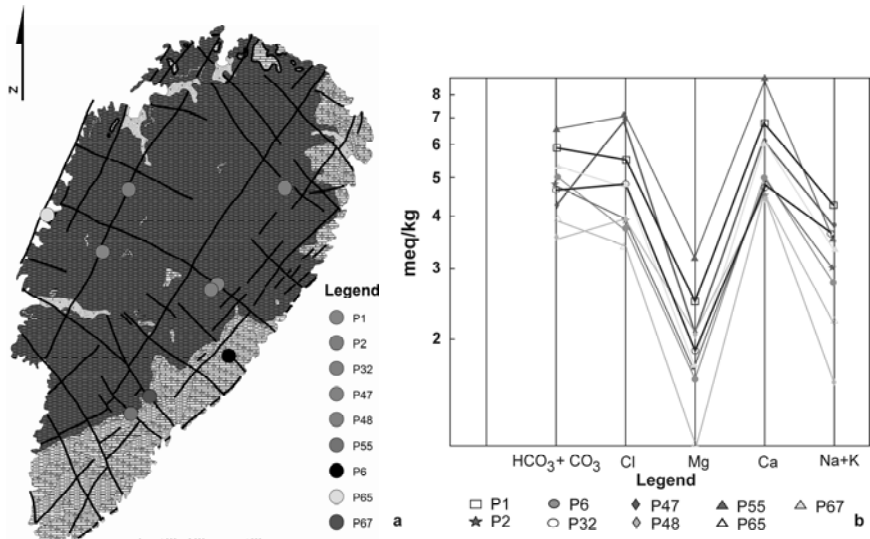


**Fig. 2.** a. Location of the main springs along the SE and SW part of the island. b. Schoeller diagram for the spring water analysis.

The groundwater hydrochemical analysis results are categorized according to the Chebotarev (1955) hydrochemical facies system. The estimated percentages of each parameter represented into the Chebotaref system for the determination of the each spring water type.

**Table 1.** The water types determined according to the Chebotaref system (1955).

| Type of water        | Clase of Springs water | Na+K (%) | Ca (%) | Mg (%) | Cl (%) | SO <sub>4</sub> (%) | HCO <sub>3</sub> +CO <sub>3</sub> TDS (%) |
|----------------------|------------------------|----------|--------|--------|--------|---------------------|---|
| Chloride-Bicarbonate | II P1                  | 27.55    | 14.38  | 3.15   | 20.6   | 4.43                | 45.16                                     |
| Bicarbonate          | I P2                   | 10.37    | 14.50  | 3.06   | 2.07   | 2.74                | 47.43                                     |
| Bicarbonate-Chloride | II P6                  | 9.87     | 15.3   | 2.97   | 20.36  | 2.89                | 48.56                                     |
| Bicarbonate-Chloride | II P32                 | 12.61    | 13.6   | 3.19   | 24.15  | 3.97                | 42.42                                     |
| Chloride             | V P47                  | 11.38    | 15.6   | 3.2    | 31.47  | 4.49                | 33.73                                     |
| Bicarbonate-Chloride | II P48                 | 6.96     | 16.7   | 4.62   | 25.99  | 4.96                | 40.74                                     |
| Chloride Sulfate     | IV P55                 | 7.99     | 16.8   | 3.7    | 24.2   | 7.05                | 40.17                                     |
| Bicarbonate          | I P65                  | 9.49     | 16.9   | 2.43   | 21.9   | 4.79                | 44.4                                      |
| Bicarbonate-Chloride | II P67                 | 10.16    | 15.87  | 2.73   | 22.2   | 4.57                | 44.3                                      |

The springs P2 and P65 belong to I Class of water (higher hydrochemical zone), which is characterized of  $\text{HCO}_3\text{-CO}_3$  water, low TDS and high flow. Spring P65 displays high scores in Chloride, apparently due to its location near the coastal zone where the sea-intrusion is possible. Springs P6, P32, P48, P67 and P47 belong to II Class of water (lower hydrochemical zone), which is characterized of low flow with Chloride character, as a result of the sea intrusion. Spring P55 belong to the intermediate hydrochemical zone which is characterized by the high degree of TDS, and moderate groundwater flow. Spring P55 belongs into the intermediate hydrochemical zone with high degree of  $\text{SO}_4$  and  $\text{HCO}_3$ . It is positioned on marble intercalations nearby the coastal area. Spring P1 belongs to the intermediate hydrochemical zone with a high degree of TDS and  $\text{HCO}_3\text{-CO}_3$  character.

## 4 Fracture Pattern extraction

Lineament orientation and lineament density distribution can play an important role in groundwater exploration or productivity analysis. One of the most convenient methods of understanding and analyzing the fracture pattern of a selected area is the interpretation of remote sensing data. Several techniques of data fusion with various spectral and spatial characteristics have been applied to Kea island aiming to the generation of different scale lineament maps.

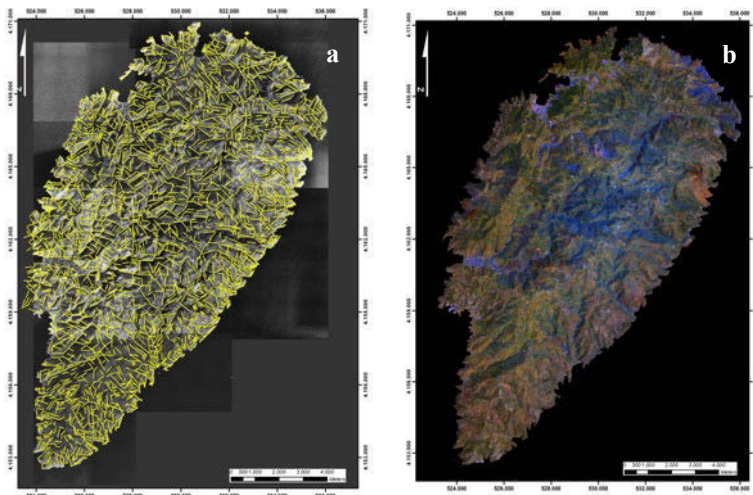


**Fig. 3.** a. Lineament map over the ortho-mosaic of aerial photos. b. An example of a pseudo-color (7,5,4/R,G,B), spatial enhanced (12) image of Kea Island, which was used -among others- for the lineament map generation.

A 25 meter resolution DEM (produced by the 20 m contours of 1:50,000 topographic maps) was used for the ortho-rectification of a Landsat-7 ETM+ scene (182/34, 30-6-2000) on a high resolution mosaic of panchromatic ortho-air-photographs, with the aid of Erdas Imagine 2010 software (Vassilakis 2006). Several color composite high resolution images were interpreted, with different band combinations and a set of lineament maps has been generated, comprising a lineament distribution map, a lineament density map and a lineament cross-point intersection density map (Botsialas et al. 2005) (Fig. 3).

## 5 Orientation of fractures

The study of the fracture orientation is fundamental, for the study of ground water flow (Stournaras et. al. 2007). As it can be seen from the rose diagrams of Figure 4, a great number of orientations characterize the lineaments pattern, mainly reflecting the complex combination and interaction between the different scale tectonic structures. Four equivalent major orientations prevail in the hydrogeological group of marbles with intercalation of gneiss-schist (NNE-SSW, NE-SW, E-W and NW-SE), whereas in gneiss-schist group one major N-S trending set and three subsidiary NE-SW, E-W and NW-SE trending sets can be observed.

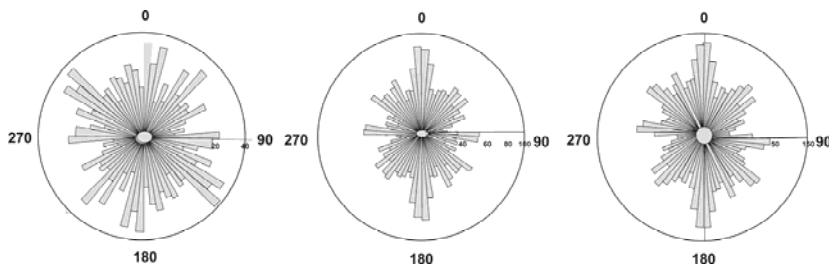


**Fig. 4.** Lineament rose diagrams for the two main hydrogeological groups (marble, gneiss-schist) and the whole island.

Since the most of the lineaments could be mainly correspond to conjugate sets of faults and fractures, we can correlate them with the dominant NE-SW dome like structure of the island and the NE-SW ductile structures (i.e. stretching lineation) that accompanied the main, green-schist facies, metamorphic event. The analysis of the whole island lineaments rose diagram show that the four major sets are oriented parallel, normal and in  $\pm 45^\circ$ , angle to the NE-SW dominant symmetamorphic structure direction.

## 6 Dimension of fractures

Fractures dimensions such as aperture and apparent aperture, are very difficult to be defined in terms of spatial analysis. Additionally, the effect of depth on the aperture makes its measurement even more complicated. The groundwater flow is being affected in a high degree by the length of the lineaments (Fig. 5).

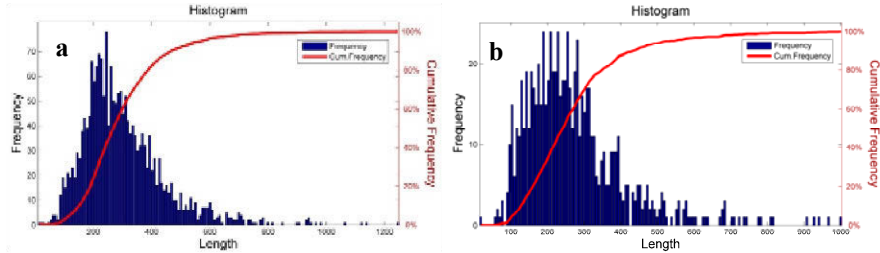


**Fig. 5.** Lineaments Length Size histograms, of gneiss-schist (a), and marble (b) dominated areas.

The length variations depend on the trends that exerted on the formations and moreover the magnitude of the erosion. The fracture map reveals lengths of surface traces between 15m and 1km at the marble dominated area. On the other hand the lineament length in gneiss-schist group varies between 9 m and 1.25 km.

## 7 Fracture Frequency and Fracture Intersection Density

Density maps represent the total number of lineaments per square kilometer area (Fig. 6a). The density varies from high to very high in the eastern side of the island, where marbles are cropping out. At the western side of the island, where gneiss-schist formation is the dominating lithology, the density varies from moderate to very high. Consequently the density map of lineament intersection points was derived, in which the frequency of intersection points per square kilometer, is illustrated (Fig. 6b).

Both, marbles and gneiss-schist mass, show a wide variety of the degree of interconnection. It is clear that the higher the density, the higher is the degree of interconnection. It is also easily observed, from the Fractures Interconnection Map, that there are two zones of high density, one in the eastern side of the island and another in the western, that represent the most internal areas of the detachment footwall with more systematic expression of the brittle tectonism.

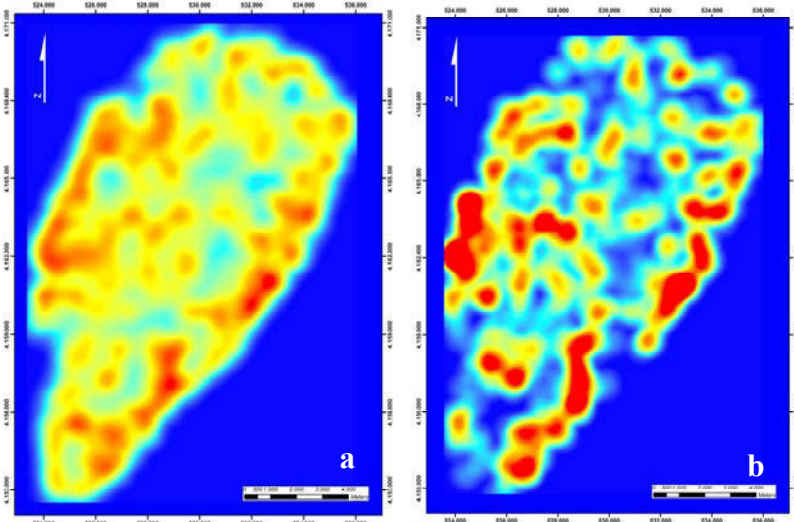


**Fig. 6.** a. Lineament Density Map. b. Fracture Intersection Density map.

## Conclusions

The main lineament orientations, extracted from the pattern analysis of remote sensing data, coincide with five major sets in the marble dominated hydrogeological group (trending NNE-SSW, NE-SW, E-W and NW-SE). Besides a major N-S trending set and three minor, NE-SW, E-W and NW-SE trending sets characterize the gneiss-schist group.

The groundwater flow occurs in various levels into the crystalline complex of Kea Island. There is a very close relation between the origin of these levels and the tectono-stratigraphic and deformational structure of the island. This structure is characterized by the alternation of higher compact and low-fragmentation petrographic masses with highly fractured and cataclastic deformed zones. The deeper level of aquifer development is expected to be the sea level. The groundwater which flows at low depth into the crystalline-schist mass of the island characterized by a high quality and low conductivity  $\text{HCO}_3\text{-CaMg}$  water type. Most springs belong into the lower hydrochemical zone in which the flow is very low with high Bicarbonate-Chloride character. The groundwater is not only karstic because during the flow path it crosses gneiss-schist horizons and as a result of that these enrich the groundwater and degrade the water quality. The search is still being processed and the results of the satellite images lineament pattern analysis is correlated with the detail field work and the study of the brittle deformation of the island. This approach is necessary for understating and interpreting the relation between the hydrochemical and hydrolithological conditions and the way that the fracture pattern of fissured rocks affects the groundwater storage and flow.



## References

- Altherr R, Kreuzer RH, Wendt I, Lenz H, Wagner GA, Keller J, Harre W, Hohndorf A (1982) A Late Oligocene/Early Miocene high temperature belt in the Attic-Cycladic crystalline complex (SE Pelagonian, Greece). *Geol. Jah.* E23, 97-164
- Botsialas K, Vassilakis E, Stournaras G (2005) Fracture pattern description and analysis of the hardrock hydrogeological environment, in a selected study area in Tinos Island, Hellas. *Proc. of 7th Hell. Hydrogeol. Conf.*, Athens, 91-100
- Chebotarev IJ (1955) Metamorphism of natural waters in the crust of weathering. *Geoch. and Cosmoch. Acta*, Vol. 88, 22-48
- Davis E. N (1982) Geological Map of Greece, scale 1:50.000, Kea Island Sheet. *Inst Geol and Miner. Explor.*, Athens
- Durr S, Altherr R, Keller J, Okrusch, M, Seidel, E (1978) The median Aegean crystalline belt: stratigraphy, structure, metamorphism, magmatism. In: Cloos, H., Roeder, D. and Schmidt, K. (eds). *Alps, Apennines, Hellenides*, 455-477, Schweitzerbart, Stuttgart
- Iglseder C, Grasemann B, Schneider DA, Lenauer I, Rice AHN, Nikolakopoulos KG, Tsombos PI, Müller M, Voit, K (2009) Characteristics of low-angle normal fault formation on Kea (Western Cyclades, Greece). *Trabajos de Geologia, Univ. de Oviedo*, 29, 372-374
- Liati A, Skarpelis N, Pe-Piper G (2007) Late Miocene magmatic activity in the Attic-Cycladic Belt of the Aegean (Lavrion, SE Attica, Greece): implications for the geodynamic evolution and timing of ore deposition. *Geol. Mag.*, Sept. 2009, 146, 5, 732-742
- McKenzie D (1978) Active tectonics of the Alpine-Himalayan belt: the Aegean Sea and surrounding regions. *Geophys. J. R. Astron. Soc.*, 55, 217-54
- Müller M (2009) Structural Investigations/Observations along a Low-angle Normal Fault and their Implication for the Geology on Northwest Kea – Examining a Major Shear Zone. *Diplomarbeit, Universität of Wien*
- Stournaras G (2008) Hydrogeology and vulnerability of limited extension fissured rocks islands. *Ecology & Hydrobiology* Vol. 8, No 2-4, 391-399
- Stournaras G, Alexiadou MCh, Leonidopoulou D (2003) Correlation of hydrogeological and tectonic characteristics of the hardrock aquifers in Tinos Island (Aegean Sea, Hellas). *Intern. Conf. on Groundwater in Fract. Rocks, Prague, Abstracts*, p. 103
- Stournaras G, Migiros G, Stamatis G, Evelpidou N, Botsialas K, Antoniou B, Vassilakis E (2007) The fractured rocks in Hellas. In: Krasny J., Sharp J. (eds.), *GROUNDWATER IN FRACTURED ROCKS*, Volume 9, Taylor & Francis, p. 133-149
- Vassilakis E., (2006) Study of the tectonic structure of Messara basin, central Crete, with the aid of remote sensing techniques and G.I.S., PhD thesis, pp.546, Athens, National and Kapodistrian University of Athens
- Yannatos G. (2003) Groundwater flow controlled by the discontinuities in fissured rocks. Two case histories. (Preliminary Announcement), 1<sup>st</sup> Workshop on Fissured Rocks, Hydrogeology proceedings, Tinos Greece